JOURNAL OF GEOPHYSICAL RESEARCH, VOL. 103, NO. C3, PAGES 5595-5606, MARCH 15, 1998

Simulation of sea ice transport through Fram Strait: Natural variability and sensitivity to forcing

Markus Harder, Peter Lemke, and Michael Hilmer

Institut für Meereskunde an der Universität Kiel, Kiel, Germany

Abstract. The interannual variability of the sea ice transport through Fram Strait is simulated with a dynamic-thermodynamic sea ice model. Forcing with daily varying wind fields for the 7-year period 1986–1992 causes a high variability of sea ice drift on timescales from days to years. Annual means of simulated ice transport through Fram Strait differ up to a factor of 2. Additional sensitivity studies investigate the response of sea ice transports to variations of the prescribed atmospheric and oceanic forcing. Wind speed, ocean current speed, air temperature, and precipitation rate are systematically varied over a wide range. The model predicts an almost linear relation of ice transport with wind speed and ocean current, a strong, nonlinear relation with air temperature, and a rather small sensitivity to changes in precipitation. The results show that the interannual variability of wind forcing causes considerable variations of sea ice export through Fram Strait. The fluxes of freshwater and negative latent heat associated with the sea ice transport can significantly affect the ocean circulation in the Greenland Sea and in the North Atlantic. This shows how variations of the ocean circulation are coupled to the variability of the atmosphere by the mechanism of sea ice advection. To adequately represent these important interactions in the coupled system atmosphere–cryosphere–ocean, both the dynamics and the thermodynamics of sea ice must be included in climate models.

1. Introduction

Sea ice plays an important role in the climate system because of the high albedo for shortwave radiation, the thermal insulation that significantly reduces the heat flux from the ocean to the atmosphere, and the storage and transport of freshwater and negative latent heat. Sea ice export from the Arctic Ocean through Fram Strait into the Greenland Sea in the order of 0.1 Sv [*Aagaard and Carmack*, 1989], compared with river runoffs, is the second largest freshwater flux on Earth, exceeded only by the Amazon. The ice outflow through Fram Strait affects the North Atlantic circulation, one of the most important regions for the global conveyor belt and the whole climate system.

To understand global climate dynamics, it is therefore nescessary to know the extent of sea ice export out of the Arctic, its natural variability, and its sensitivity to changes of the forcing. So far, only few, scattered observations are available for estimates of the ice transport through Fram Strait. Time series of these measurements usually cover only some months, hardly allowing investigations on the long-term natural variability of the ice export. Additionally, little is known about the response of the ice export to variations in atmospheric forcing associated with natural or anthropogenic climate changes. A review of previous investigations is given in a separate section.

Numerical models can partially fill the gap caused by the lack of observations, and give estimates of the modified role of sea ice under changing climatic conditions. The focus of this paper is to present the results of a large-scale numerical simulation of sea ice in the northern hemisphere with respect to sea ice transports, associated net freezing rates, and fluxes of freshwater and negative latent heat.

The natural variability of ice exports caused by interannual variations of the wind field is analyzed with a dynamic-thermodynamic sea ice model. Additionally, sensitivity studies for 33 situations are carried out to investigate the response of the simulated ice transports to changes of the atmospheric forcing. Wind speed, ocean current, air temperature, and precipitation rate are systematically varied over a wide range covering the expected spectrum on climatological timescales.

Paper number 97JC02472.
0148-0227/98/97JC-02472$09.00

2. Model Description

2.1. Sea Ice Physics

The dynamic-thermodynamic model considers sea ice a two-dimensional continuum described by the mean ice thickness (ice volume per area) h, the ice concentration

(areal coverage) A, and the ice drift velocity $\mathbf{u}$. It is based on the viscous-plastic model of *Hibler* [1979] with the thermodynamics following *Parkinson and Washington* [1979]. Several improvements regarding ice dynamics have been made: an upstream advection scheme to avoid negative ice thicknesses, no explicit diffusion, and drag coefficients optimized by comparison with observed buoy drift [*Harder and Lemke*, 1994; *Fischer*, 1995; *Drinkwater et al.*, 1995; *Harder*, 1996; *Kreyscher et al.*, 1997].

The evolution of the ice cover is given by the extended continuity equations

$$\frac{\partial h}{\partial t} + \nabla \cdot (\mathbf{u}h) = S_h \tag{1}$$

$$\frac{\partial A}{\partial t} + \nabla \cdot (\mathbf{u}A) = S_A \tag{2}$$

where S_h and S_A are the thermodynamic source and sink terms. S_h is determined from an energy budget at the ice surface (including shortwave and longwave radiation, parametrization of clouds) following *Parkinson and Washington* [1979] and the zero-layer approximation of *Semtner* [1976] for the heat conduction through the ice. S_A is parametrized as an empirical function of S_h as described by *Hibler* [1979]. The ice concentration A is not allowed to exceed unity.

A prognostic snow layer according to *Owens and Lemke* [1990] is also included. The evolution of the snow cover is determined from the additional extended continuity equation

$$\frac{\partial h_s}{\partial t} + \nabla \cdot (\mathbf{u}h_s) = S_s \tag{3}$$

Here h_s is the mean snow thickness (snow volume per area) analogous to the mean ice thickness h. S_s represents the sources and sinks of snow on the ice. Prescribed precipitation rates are the source of snow. Only precipitation over areas covered with sea ice and with surface air temperatures below the freezing point is assumed to add to the snow cover.

The sink term for the snow is the same energy balance at the upper surface of the ice floe as used for the mean ice thickness h, except that the albedo takes a different value. It is assumed that the snow cover on an ice floe must totally melt before the ice starts to melt. That is, when the energy budget yields a surplus (caused by high solar radiation and warm air temperatures in summer), this excess energy reduces the snow cover, whereas the ice thickness is not yet affected. Once the snow has vanished, the excess energy melts the ice, that is, decreases the mean ice thickness h.

The ice drift velocity $\mathbf{u}$ is determined from the momentum balance

$$m\frac{D\mathbf{u}}{Dt} = \tau_a + \tau_w - mf\mathbf{k}\times\mathbf{u} + \mathbf{F} - mg\nabla H \tag{4}$$

where τ_a and τ_w are the atmospheric and oceanic drags, $-mf\mathbf{k}\times\mathbf{u}$ is the Coriolis force depending on the ice mass per area m and the Coriolis parameter f, $\mathbf{F}$ represents the internal forces of the ice, and $-mg\nabla H$ is the force due to the tilt of the ocean surface H, proportional to the gravitational constant g. A viscous-plastic rheology with an elliptical yield curve according to *Hibler* [1979] describes the internal forces $\mathbf{F}$ as the divergence of the stress tensor. Atmospheric drag is given as

$$\tau_a = \rho_a c_a |\mathbf{u}_a| \mathbf{R}_\phi \mathbf{u}_a \tag{5}$$

according to boundary layer theory [e.g., *McPhee*, 1979], and similarly the oceanic drag is described as

$$\tau_w = \rho_w c_w |\mathbf{u}_w - \mathbf{u}| \mathbf{R}_\theta (\mathbf{u}_w - \mathbf{u}) \tag{6}$$

where ρ_a and ρ_w are the densities of air and water, c_a and c_w are the drag coefficients, and $\mathbf{u}_a$ and $\mathbf{u}_w$ are wind and ocean velocities. $\mathbf{R}$ is an orthogonal matrix that describes the deflection angles between drag and velocity of the forcing medium. These angles are $\phi = 0°$ for the surface wind and $\theta = 25°$ [*McPhee*, 1979] for the geostrophic ocean current.

Values for drag coefficients are $c_a = 2.2 \times 10^{-3}$ for the wind and $c_w = 5.5 \times 10^{-3}$ for the ocean. Whereas the value of c_w, determined from measurements during the Arctic Ice Dynamics Joint Experiment (AIDJEX) [*McPhee*, 1979], is the same as used by *Hibler* [1979], c_a is significantly higher than in the *Hibler* [1979] model. Comparison of simulated ice drift with buoy data [*Harder*, 1994, 1997] has shown the strong effect of the ratio c_a/c_w on the ice drift. Best agreement between simulation and observations is obtained with $c_a/c_w \approx 0.4$ [*Fischer*, 1995; *Kreyscher et al.*, 1997] as applied here.

Sea surface tilt ∇H is derived from the ocean current $\mathbf{u}_w$ via geostrophy. This small term in the momentum equation has minor effects in the simulation and is included only for completeness. The same is true for the inertia term $mD\mathbf{u}/Dt$ on the left side of the momentum equation (4), as long as timescales not shorter than a day are considered.

2.2. Model Grid and Forcing

The model is run on a rotated spherical grid covering the whole Arctic with a spatial resolution of 1° (approximately 110 km). Distortion of the shape of the grid cells from ideal squares is minimized by laying the model equator through the geographical north pole, with the model's north pole in the Indian Ocean at 0°N 60°E in geographical coordinates. A daily time step is applied.

Atmospheric forcing fields (wind, air and dew point temperatures) are derived from the surface data set of the 6-hourly European Centre for Medium-Range Weather Forecasts (ECMWF) global analyses of the seven years 1986–1992. The ECMWF wind field, av-

eraged to daily mean values, shows a realistic representation of synoptic events and a good agreement with observations. The ECMWF analyses use the pressure measurements of ice drift buoys in polar regions, many of them deployed in the framework of the International Arctic Buoy Program (IABP). They provide for a fairly realistic pressure field, and thus for good estimates of the geostrophic wind. *Hilmer* [1997] compares the 2-m wind field of the data assimilation models of two different weather services: the ECMWF analyses and the National Centers for Environmental Prediction (NCEP)/National Center for Atmospheric Research (NCAR) reanalyses. On a monthly base, the wind fields are very similar. This is not unexpected because both models use the same pressure data from ice buoys. Even on a daily base, both models yield similar wind fields, except that the exact locations of lows and highs differ in some cases. Also, some qualitative comparisons of the ECMWF wind field with measurements on board R/V *Polarstern* on cruises in polar oceans in both hemispheres have been made (M. Kreyscher and M. Windmüller, personal communication, 1997). Although the measurements at more than 30 m height are not directly comparable with the 2-m wind analyses, a generally good agreement of wind speed and direction in model and analyses has been found.

Further, the comparison of the simulated ice drift with observed ice buoy drift shows that the ECMWF wind field is realistic. *Kreyscher et al.* [1997] and *Lemke et al.* [1997] compare the statistics of the simulated ice drift with observations of about 200 IABP buoys in 1986–1992. They use the same model forced with 2-m ECMWF winds as applied here. It is found that the viscous-plastic sea ice model reproduces the observed drift speed statistics well. *Harder* [1997] shows a comparison of simulated ice drift trajectories with nine observed IABP buoys. The model is able to reproduce the trajectories over periods as long as 1 year, with no information from the buoy observations helping the model. A similar comparison of simulated ice drift with the observed trajectory of Ice Station Weddell 1 is shown by *Drinkwater et al.* [1995]. The same model and the same ECMWF wind forcing are used, but here applied to the Southern Ocean. Similar to the Arctic, the model reproduces the observed ice drift well. In summary, several comparisons with observations indicate that the simulated ice drift forced with ECMWF winds is reasonable, and that the ECMWF wind field matches the measurements obtained from ice buoys, ships, and ice stations.

This does not hold true for the ECMWF air and dew point temperatures at 2 m height. Figure 1 shows the time series of ECMWF air temperature at the north pole as a representative example for ice-covered regions. Because ECMWF prescribes climatological monthly mean temperatures for sea ice surfaces without using the buoy temperature measurements, the 2-m temperatures in polar regions are basically held constant within each month, with artificial steps up to 10°C at the beginning of a new month. The summer period with temperatures close to the freezing point lasts for an unrealistic long period of 3 months (June 1 to August 31), whereas the observed summer period [*Colony et al.*, 1992] lasts only about 2 months (June 15 to August 15). Mean summer air temperatures over sea ice are decreasing from a realistic 0°C in 1986 to an unrealistic −2°C in 1992.

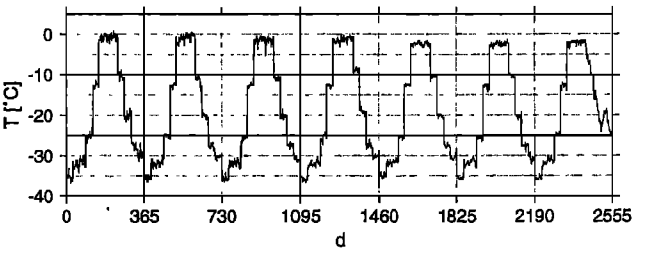

Figure 1. Time series of the surface air temperature at 2 m height at the north pole in the analyses of the ECMWF model for the period 1986–1992.

To remove these undesirable effects due to changes in the ECMWF model, a correction for the ECMWF air and dew point temperatures is applied. Seven-year mean temperatures are calculated for each month of the year. Daily values are linearly interpolated between the corresponding monthly means. In the summer period from June 15 to August 15, air temperatures are not allowed to fall below 0°C. Dew point temperatures are adjusted accordingly so that the relative humidity of the air is conserved.

This correction of ECMWF temperatures provides a reasonable quasi-climatological seasonal cycle without any interannual variability. Also, the prescribed annual mean ocean currents do not vary interannually. This limits the investigation of interannual variability here to variations in the wind field. Sensitivity studies, however, can be performed with respect to changes in wind and ocean current speed, air temperature, and precipitation.

Precipitation rate and cloudiness are described as spatially constant, climatological monthly means. Daily values are derived by linear interpolation. Precipitation data are taken from *Vowinckel and Orvig* [1970], cloud data from *Ebert and Curry* [1993]. The mixed layer is described by a simple one-dimensional model with a fixed mixed layer depth of 25.4 m. Spatially varying, temporally constant ocean currents and oceanic heat fluxes are taken from the coupled ice–ocean model of *Hibler and Zhang* [1994]. The oceanic heat flux varies between 1–2 W m^{-2} in the central Arctic up to more than 100 W m^{-2} in the eastern Greenland Sea.

3. Standard Simulation

In this section the simulation results regarding ice thickness, snow thickness, ice drift, and net freezing rate are presented.

The standard simulation integrates the model equations for 21 years, using three cycles of the 7-year forcing data from 1986–1992. Starting with an ice-free ocean, the model runs 14 spin-up years to reach a cyclostationary state, then another 7 years to obtain the simulation results. Only the last 7-year period, which does not significantly depend on the initial conditions, is considered here.

Figure 2 shows the simulated mean ice thickness h in March 1992 as an example for the situation at the end of winter. Highest ice thicknesses exceeding 6 m are predicted north of Greenland and the Canadian Archipelago. Lowest values occur north of Siberia over the Eurasian Shelf, covered with ice about 2 m thick. A similar spatial distribution is found in summer (see Figure 3 for August 1992), but with ice thicknesses generally decreased by about 1 m. Large areas over the Eurasian Shelf are ice-free or covered with (on average) very thin ice.

The overall pattern is in reasonably good agreement with the observations shown by *Wadhams* [1994] and by *Bourke and McLaren* [1992]. A simulated sea ice thickness of about 4 m at the north pole also agrees with the measurements evaluated by *McLaren et al.* [1994]. A more quantitative validation of these model results is given by *Kreyscher et al.* [1997].

Figure 4 displays the contours of simulated snow thickness h_s for April 1992. The snow cover reaches its highest thickness at about this time at the end of winter. Snow thicknesses are in the range of 10–40 cm with a gradient from highest values north of Greenland to lowest values north of Siberia. The snow cover melts almost totally in summer. These model results agree with the observations shown by *Barry et al.* [1993] and *Tucker et al.* [1987].

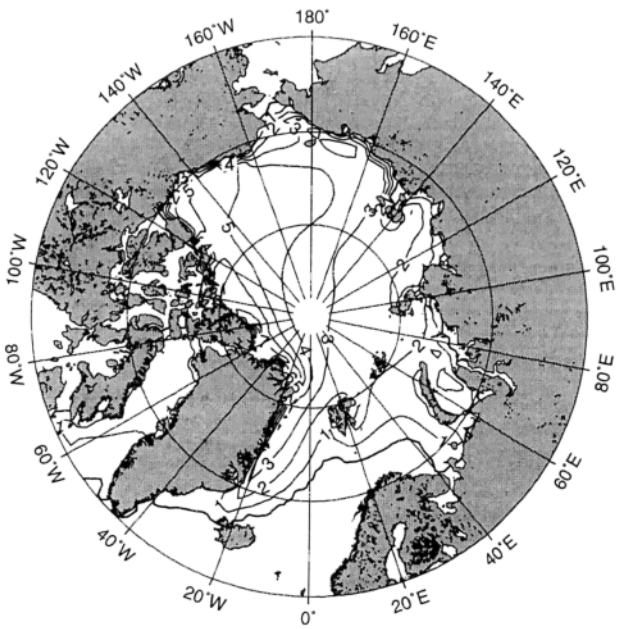

Figure 2. Simulated mean ice thickness (meters) in March 1992.

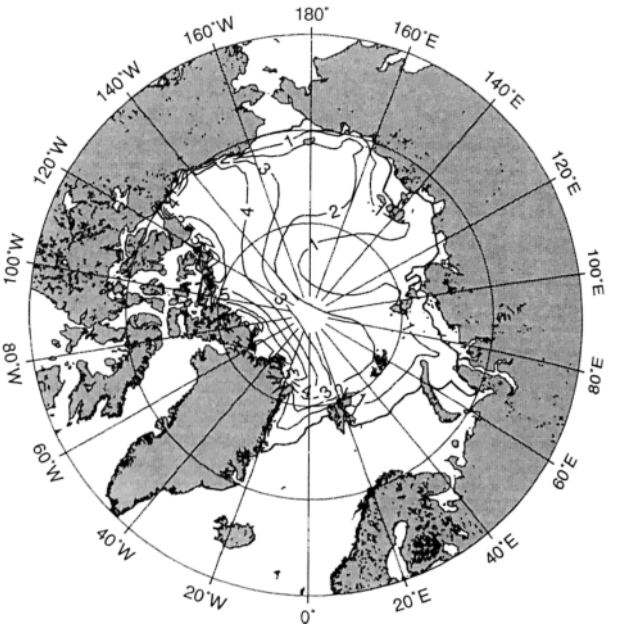

Figure 3. Simulated mean ice thickness (meters) in August 1992.

The annual mean of the ice drift speed in 1989, which is the year with the strongest ice export in this simulation, is shown in Figure 5. A mean transport of sea ice from the Siberian region toward Greenland and further on through Frams Strait can be clearly seen. It must be kept in mind that this annual mean drift is the long-term result of strongly varying daily winds, with the ice drift on the timescale of days and weeks often strongly deviating from the annual mean.

Additionally, the interannual variability of ice drift velocities is high. This can be seen from Figure 6, which shows the simulated annual mean drift in 1987, a year with a weak simulated ice export. Again, a mean transport occurs from the Eurasian Shelf regions to Fram Strait. By comparing Figure 5 and Figure 6, variations in the strength and direction are found even for the annual mean drift. In 1987, the Beaufort Gyre visible in the ice drift is much more pronounced than in 1989, whereas the year 1989 shows a very broad and strong ice transport in the Transpolar Drift toward Fram Strait. This high variability of sea ice drift is also found for the other years of the simulation.

A characteristic pattern of regions with net freezing or net melting is established as a result of the long-term transports of sea ice with ice drift on timescales of months and years. Figure 7 shows the spatial pattern of the net freezing rate (meters of sea ice locally frozen per year) as the mean value of all seven years in the simulation. Highest values over 1 m per year are found in the Eurasian region with seasonal ice cover, whereas moderate but still recognizable freezing in the central Arctic with thick, perennial ice is predicted. This gradient occurs because the heat transfer from the ocean to the atmosphere is significantly higher for open water than for ice-covered sea. Negative values of the net

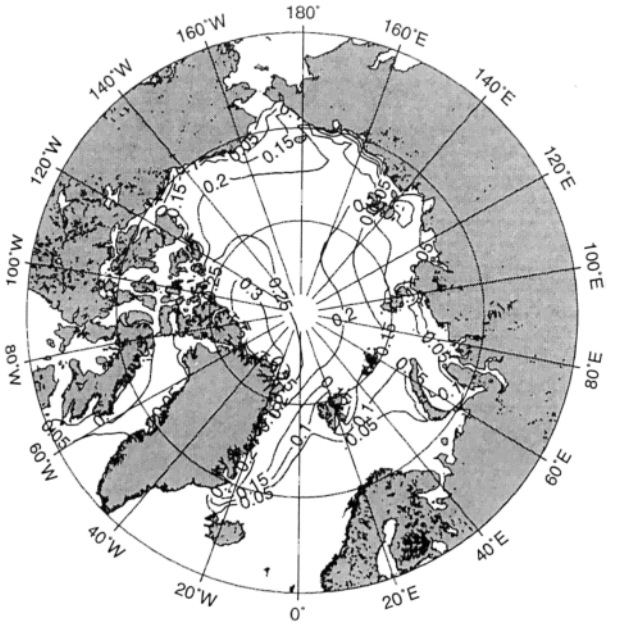

Figure 4. Simulated mean snow thickness (meters) in April 1992.

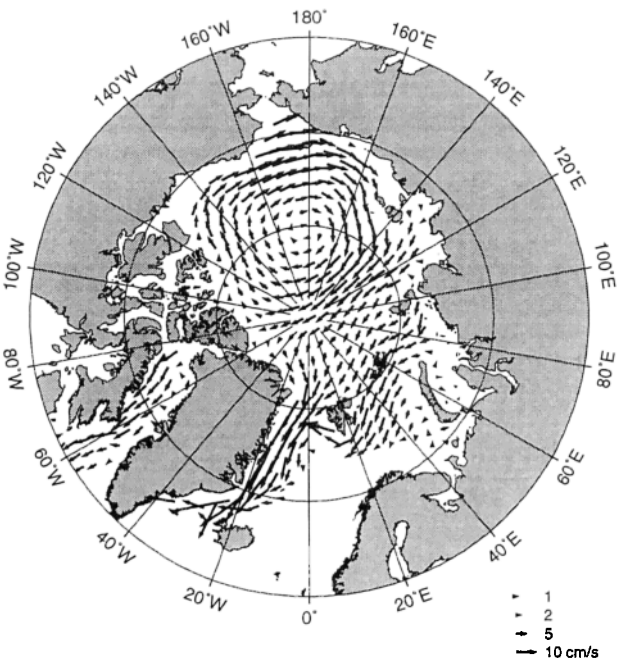

Figure 6. Simulated mean ice drift velocity in 1987.

freezing rate, exceeding 3 m per year, are found in the Greenland Sea. They indicate a strong long-term mean melting of sea ice in this region, associated with a considerable input of freshwater and negative latent heat into the oceanic mixed layer.

Most of the ice transport from the freezing regions north of Siberia to the melting regions in the Greenland Sea passes through Fram Strait. Thus, the flux of sea ice through Fram Strait is an appropriate measure of the ice export out of the Arctic Ocean. As the ice drift velocity has been shown to have a significant long-term variability, associated ice transports must be expected to show a similar variability, investigated in the following.

4. Exports and Interannual Variability

The sea ice transport T through Fram Strait is calculated for an almost zonal section S consisting of four aligned model grid cells at about 80°N from the north-

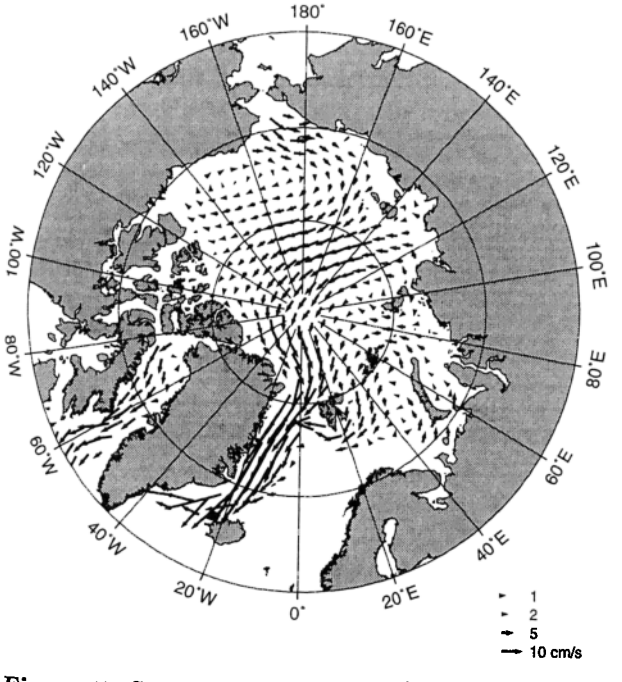

Figure 5. Simulated mean ice drift velocity in 1989.

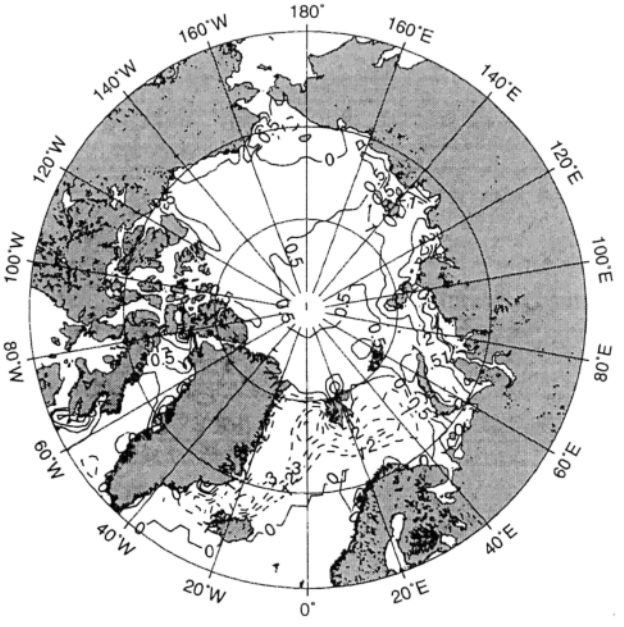

Figure 7. Simulated growth rate (meters per year) of sea ice for the period 1986–1992. Negative values indicate melting.

eastern tip of Greenland to the northwestern tip of Spitsbergen as

$$T = \int_S u_\perp(\mathbf{x})\, h(\mathbf{x})\, d\mathbf{x} \qquad (7)$$

where $\mathbf{x}$ is the position along the section, $u_\perp$ is the southward ice drift component perpendicular to the section S, and $h(\mathbf{x})$ is the mean ice thickness (mean floe thickness times areal coverage). T is a volume flux given in sverdrups (1 Sv=10^6 m^3 s^{-1}) or km^3 per year.

The resolution of the model of about 110 km limits the accuracy of the simulated ice transport through Fram Strait, which is represented by four grid cells. On the other hand, this resolution allows the simulation to be run on a large model grid covering the whole Arctic over long time periods. Additionally, the relatively small CPU time required by the model (1 hour on a fast workstation for the standard simulation) allows many simulations to be run with systematically varied boundary conditions as shown in the sensitivity studies below.

Southward transport of sea ice through Fram Strait is calculated for every day of the 1986–1992 period. These daily data combine two effects. First, the transport is proportional to the mean ice thickness h as a result of long-term thermodynamic and dynamic ice buildup on timescales of months and years. Second, the transport is proportional to the actual southward ice drift speed $u_\perp$ with a high-frequency variability caused by the wind field on synoptic timescales of the order of days.

As the focus here is the investigation of interannual variations, the high-frequency variations are smoothed out by calculation of monthly mean exports for the 84 months of the simulation. This is the basis for the following analyses. The variability on timescales of months and years is fully included in the monthly averages. Single synoptic events that may move the ice northward one day and southward the next day are only considered as far as they contribute to the long-term sea ice transport.

Seven-year means of sea ice export are calculated for each month of the year in order to distinguish between seasonal and interannual variations. Figure 8 shows this mean annual cycle. The seasonal variation with highest exports in winter, when the ice is thick and the driving storms are strong, is clearly visible.

Interestingly, a dip related to sea ice rheology occurs in January and February. In the midst of winter, the sea ice becomes thick and very compact. This increases the internal forces associated with ice deformation, which tend to reduce the ice velocity and thus the ice outflow. At the beginning and the end of the winter, when the ice is less compact, outflow is possible with less resistance.

The 7-year mean ice volume export, that is, the annual average of the mean seasonal cycle of Figure 8, is 0.0855 Sv, or 2696 km^3 per year. This sea ice export out of the Arctic Ocean is associated with a transport of negative latent heat into the Greenland Sea of the order of 20 TW, a considerable contribution to the energy balance of this region.

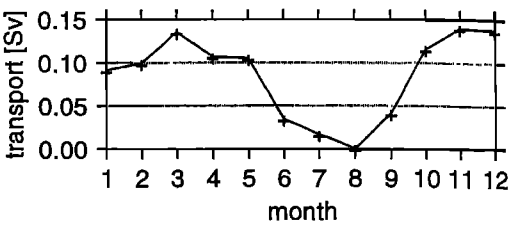

Figure 8. Simulated mean seasonal cycle of sea ice transport (sverdrups) through Fram Strait at 80°N for the period 1986–1992.

Considering the freshwater flux associated with this sea ice transport, it must be kept in mind that the density of sea ice (approximately 900 kg m^{-3}) is somewhat lower than that of seawater, and that sea ice is not pure freshwater but includes some salt, resulting in a salinity of a few practical salinity units for sea ice. Thus, values for freshwater fluxes with ice drift are some 10–20% smaller than the sea ice volume transports calculated here.

Long-term observations of sea ice transports through Fram Strait needed to estimate the variability require simultaneous observations of ice thickness, areal ice coverage, and ice drift. In practice, these variables are often measured with different types of sensors and evaluation methods (satellite data, upward looking sonars on moorings) at different locations and different times and with differing resolution. Periods of really simultaneous observations rarely exceed some months. This shows the need for enhanced efforts to acquire long-term observations of the ice transports.

At the present stage, the natural variability of these sea ice transports can be investigated with numerical models. Figure 9 shows the simulated monthly anomalies of sea ice transport through Fram Strait for each of the 84 months of the 7-year period 1986–1992. Anomalies are defined as deviations of the mean transport for a specific month from the 7-year mean value for this month of a year (shown in Figure 8).

Remarkably, the anomalies of monthly ice transports (Figure 9) are of the same order of about 0.1 Sv as the long-term mean transport. These anomalies are solely caused by fluctuations in the wind field, which is the only, but most important, daily and interannually varying forcing variable in this simulation.

Integrating the monthly mean ice exports to annual means for each of the seven years 1986–1992 (Figure 10) makes the high interannual variability even more clearly visible. For example, the annual mean export in 1989 is almost twice as large as in 1987. The standard deviation of the annual means with respect to the 7-year mean value of 0.086 Sv is 0.018 Sv, or 21%.

Whereas the absolute long-term value of the simulated mean ice exports depends on the accuracy of the model forcing as well as on the proper choice of model

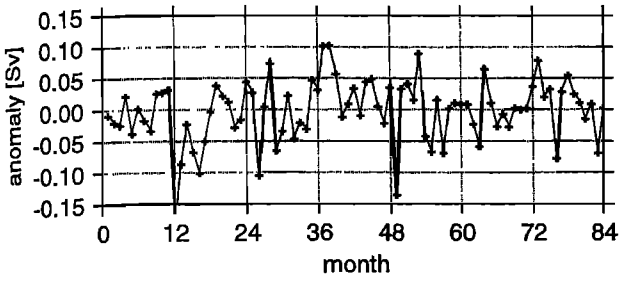

Figure 9. Simulated monthly anomalies of sea ice transport (sverdrups) through Fram Strait at 80°N for the period 1986–1992.

parameters, the important result of the high variability on timescales of months and years is much less sensitive. The high variability of sea ice export through Fram Strait, expressed as the ratio of its standard deviation by the long-term mean value, does not significantly vary with changes in forcing fields or model parameters.

5. Sensitivity to Forcing

Several simulations with varied prescribed boundary conditions have been performed to investigate the effect of variations (or errors) in the forcing fields on the simulated sea ice transport through Fram Strait. The original forcing fields are overlaid with a systematically varied disturbance signal, and the response of the prognostic variables describing the sea ice cover is investigated.

This method has some implicit restrictions. First, the disturbance signal is prescribed as spatially and temporally constant. This is a highly idealizing assumption which is neither expected nor intended to represent the reaction of the real climate system to realistic changes in the forcing. Second, the simulations are performed with a stand-alone sea ice model with fixed oceanic and atmospheric boundary conditions, that is, feedback mechanisms are neglected. Despite the limitations, these simplifications are useful. The sea ice component is subjected to a clearly defined set of varied boundary conditions. This approach is similar to the sensitivity studies of *Fischer and Lemke* [1994] for a Weddell Sea ice model. A clear, quantifiable response of the prognostic sea ice variables to the modified forcing is obtained. The various feedback mechanisms that modify or even mask the original cause–response relation in fully coupled climate models are excluded in these sensitivity studies.

The interannual variability of sea ice exports caused by fluctuations in the wind field shows the importance of atmospheric forcing for ice transports. To investigate the influence of changes in ice transports due to varied forcing, 33 different scenarios have been simulated. The four forcing variables considered are wind speed (without change in wind direction), ocean current speed (also without change in direction), air temperature, and precipitation rate.

For each of the four sensitivity studies, one forcing variable is varied while the other ones are held constant at standard values. First, the wind speed is varied in the range between 0% and 200% referring to standard wind speed, with a step size of 25%. Second, the ocean current speed is varied in the same range between 0% and 200% of its standard value, again with a step size of 25%. In a third series of scenarios, air temperatures are varied in steps of 1°C from -4°C to +4°C, compared with standard forcing. The fourth investigation considers changes in precipitation rates between 0% and 200% of the standard precipitation, again with steps of 25%.

These scenarios yield results that can be interpreted in two ways. First, the variations in forcing variables can be seen as deviations of the climate system from the present state. In this view, the experiments are regarded as investigations of previous, future, or hypothetical climate states. Second, the variations may represent errors in forcing data due to uncertainties in observations. From this viewpoint, the sensitivity studies show the magnitude of the effects of errors in the forcing functions on the sea ice simulation.

Figure 11 shows the response of sea ice exports to changes in wind speed, which is the main driving force for sea ice advection. This sensitivity study shows an almost linear correlation between ice export and wind speed, pointing out that knowledge of wind speed and

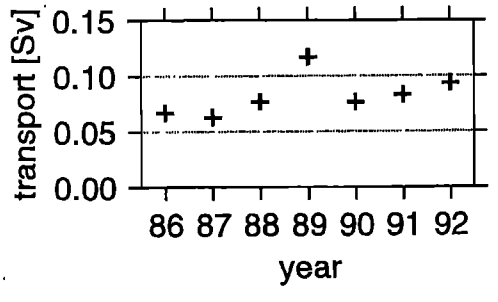

Figure 10. Annual mean sea ice transport (sverdrups) through Fram Strait at 80°N for the period 1986–1992. The 7-year mean value is 0.086 Sv with a standard deviation of 0.018 Sv, or 21%.

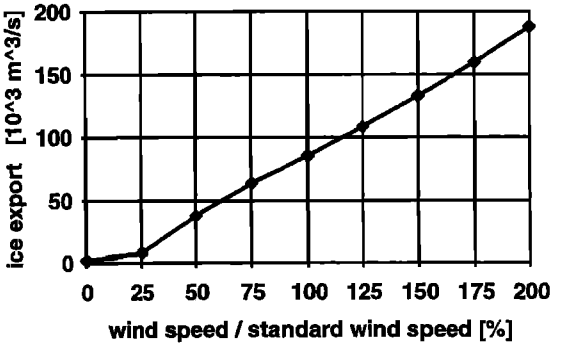

Figure 11. Sensitivity of simulated sea ice export through Fram Strait to variations in wind speed.

associated drag on the ice are very important for estimates of sea ice drift.

The proportionality between ice export and wind speed is valid for a wide range of wind speed variations. It is only for small wind speeds that the linear relation no longer accurately applies. When the wind is very weak, the wind-driven forcing can no longer overcome the resistance of the ice cover to deformation. In this case, the ice drift is dominated by ocean currents. The (annual mean) ocean drag is generally too weak to break up a compact ice cover, and thus is only active when the ice compactness is reduced and internal forces are small. When there is no wind at all and the ocean current is the only driving force, Figure 11 gives an ice export of 0.004 Sv, only about 5% of the standard simulation value. (The transport caused by ocean currents alone may be significantly larger when strong short-term fluctuations of the ocean current are included, for example, in a coupled ice-ocean model.)

The effects of variations in the magnitude of the ocean current on sea ice transport are shown in Figure 12. Similar to the effect of wind forcing, a linear relation between ocean current and ice transport through Fram Strait is found. But two striking differences, compared with variations of wind speed, are found for the ocean current speed: First, the ice transport is not zero when the ocean current is turned off. In this case, the ice transport (caused by daily wind forcing only) is still 0.0573 Sv, or 67% of its standard value. Second, the sensitivity of the ice transport on the ocean current indicated by the slope of the curve in Figure 12 is not as large as for the wind field (Figure 11). Uncertainties or changes in wind speed appear to have a larger effect on the ice transport than variations in ocean current speed. Although this study is limited by the different timescales of the applied daily winds and temporally constant ocean currents, it seems physically reasonable that synoptic weather events related to short-term variations in wind speed (and direction, which is not investigated here) have a stronger impact on sea ice dynamics than the ocean. While the atmosphere forces ice motion, the ocean has two important effects on sea ice dynamics: Ocean currents are a cause of sea ice motion, but the importance of friction in the ocean mixed layer dampening ice drift is often of the same order or even larger than the effect of driving ocean currents.

Figure 13 shows the effect of changing air temperatures on sea ice exports. There is a negative correlation: Higher temperatures reduce the mean ice thickness and areal coverage, leading to less ice export. Lower temperatures have the opposite effect. In the vicinity of the standard simulation, an increase (decrease) in air temperature by 1°C is accompanied by a decrease (increase) in ice export of the order of 30%.

When larger variations in air temperature are considered, this linear relation no longer holds true. For air temperatures below -2°C, the ice export becomes almost independent of the air temperature, and does not exceed approximately 0.15 Sv. The reason is the buildup of a compact ice cover over the whole Arctic even in summer, with the strong insulating effects of the ice compactness and thickness prohibiting further ice growth. A similar phenomenon is observed in the Weddell Sea ice model of *Fischer* [1995].

Strong increases in air temperatures up to 4°C represent the other extreme of the scenarios shown in Figure 13. Air temperatures in summer then are warm enough to melt the ice almost totally, yielding a seasonal ice cover for the entire Arctic. But in winter, the cold temperatures of about -35°C at the north pole are not substantially affected by an increase of 4°C. In this case, the ice export mainly depends on the amount of first-year ice frozen in winter, with the ice cover almost vanishing in summer.

While these simulation results are considered as important estimates of the effects of climate change, the limitations of a numerical simulation must be kept in mind. Observational data, which are presently rare, are required to verify the model results and to optimize the model parameters. Additionally, the quality of the forcing data, with the deficits shown above, must be increased [*Fischer and Lemke*, 1994].

The effects of modified precipitation rates on ice exports are shown in Figure 14. More precipitation increases the snow thickness on sea ice, reducing the mean

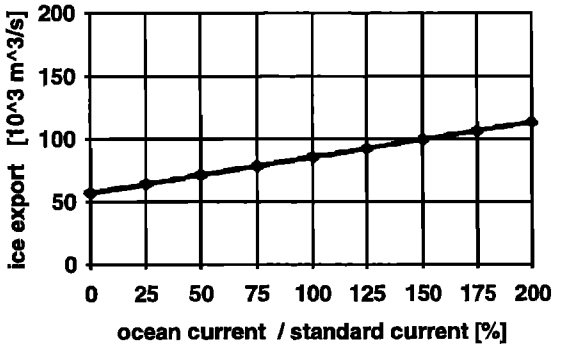

Figure 12. Sensitivity of simulated sea ice export through Fram Strait to variations in ocean current speed.

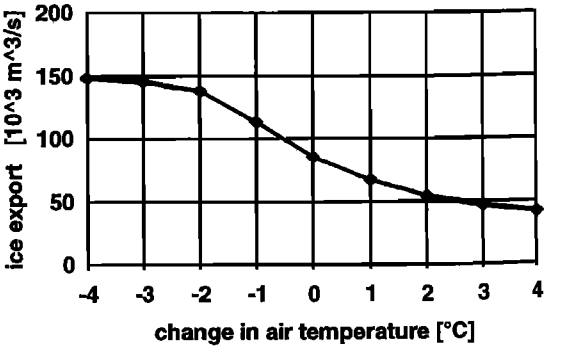

Figure 13. Sensitivity of simulated sea ice export through Fram Strait to variations in air temperature.

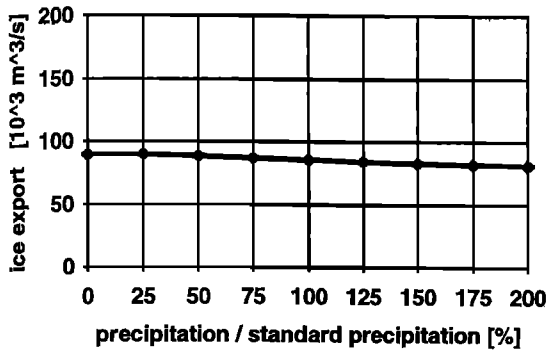

Figure 14. Sensitivity of simulated sea ice export through Fram Strait to variations in precipitation rate.

ice thickness by thermal insulation, and thus leading to lower transports. This negative correlation between precipitation rate and exports is clearly visible in Figure 14.

However, the effect of varied precipitation is relatively small. Without any precipitation, the sea ice export is increased by 9% compared with the standard simulation. Similarly, the ice export is decreased by the same amount of 9% when the precipitation is increased to twice the standard value. Thus, the model predicts that changes in precipitation rates cause only minor modifications of sea ice transports.

6. Comparison With Other Simulations and Observations

Several authors estimated the ice transport through Fram Strait from models for different periods and with different resolutions. Simulations of sea ice transport started with the dynamic-thermodynamic sea ice model of *Hibler* [1979] which has since been applied to periods from the 1950s to present. The *Hibler* [1979] model predicted a Fram Strait ice outflow of 3220 km^3 per year, or 0.10 Sv.

A numerical simulation of ice transport for the period 1951–1980 has been performed by *Walsh et al.* [1985]. The model has a resolution of 220 km and is forced with NCAR atmospheric fields given on a grid with 5° resolution. The long-term mean outflow for the years 1951–1980 has been calculated as only 0.044 Sv, which is significantly smaller than most other estimates from models or observations. Insufficiencies in forcing fields as well as in model parameters may have caused these discrepancies. *Walsh et al.* [1985, p. 4860] suggest "that the excessive summer melt in the model simulations results in unrealistically low rates of ice export during summer". This shows that absolute values of transports depend on the model configuration.

Walsh et al. [1985] find that the simulated ice volume transport through Fram Strait varies by factors of 2–3 in successive years, and the simulated summer export is only 12.2% as large as the winter export. Both results are also found in the model applied here.

First studies with the present model yielded a long-term Fram Strait ice export of 0.14 Sv for the period 1986–1992 [*Harder*, 1996]. Later it was found that the ice thickness at the north pole exceeded the observed values given by *McLaren et al.* [1994]. This was partially attributed to insufficiencies in the prescribed ocean current, and partially to inadequate model parameters (for example, ice strength, time constant for freezing of open leads). These problems have been corrected by using the ocean current from the coupled ice-ocean model of *Hibler and Zhang* [1994], and by adjusting the model parameters [*Kreyscher et al.*, 1997] so that the simulated ice thickness matches the observations. While absolute values of sea ice transport depend on the model configuration, other physical properties such as temporal variability and sensitivity to forcing variables seem to be less sensitive. The years with extraordinarily large or small exports remained the same for all simulations not too far off the standard case.

Häkkinen [1993] performs a numerical simulation of Fram Strait ice outflow with a coupled ice-ocean model for the years 1955–1975. The model of *Häkkinen* [1993] shows that anomalies in the wind forcing are a major source of extraordinarily high sea ice transport through Fram Strait in 1959, 1962, and 1968. This ice outflow supposedly caused an excessive ice cover in the Greenland Sea and related freshwater anomalies. The mean ice thickness at the north pole of less than 2 m in the simulation of *Häkkinen* [1993] is smaller than the observed climatological ice thickness of about 3–4 m [*McLaren et al.*, 1994]. *Häkkinen* [1993] suggests that the ice transport through Fram Strait and its anomalies might thus be underestimated. Although the simulation of *Häkkinen* [1993] is not for the same period as the present study, the results are in good agreement: Anomalies of the wind field are shown to cause anomalies in sea ice transports of the order of the Great Salinity Anomaly (GSA) [e.g., *Dickson et al.*, 1988; *Legutke*, 1991], and the GSA observed in the late 1960s and 1970s seems to be a regular phenomenon of the internal variability of the climate system rather than a singular event. The year-to-year variations in sea ice transport in the present simulation for 1986–1992 are of the order of 1000 km^3, about half the estimated value of the GSA [*Dickson et al.*, 1988]. Longer time series of atmospheric forcing data, especially the reanalyses from NCEP/NCAR and ECMWF, will be used in future simulations to detect the variability on decadal timescales.

A number of articles deal with related issues. The sensitivity of a dynamic-thermodynamic sea ice model and the variability on multidecadal timescales (1960–1988) has been investigated by *Chapman et al.* [1994]. *Häkkinen and Mellor* [1992] study the seasonal variability of the Arctic sea ice cover with a coupled ice-ocean model. *Holland et al.* [1993] perform a large number of sensitivity experiments with a coupled ice-ocean model. Due to the high consumption of computer time, they investigated only the extreme cases for parameter values

and for different treatment of physical processes. *Fleming and Semtner* [1991] study the effect of interannual ocean forcing in a coupled ice-ocean model. They show that the inclusion of an interactive ocean yields a significant improvement compared against a simulation with a prescribed ocean as used here. *Flato* [1995] investigates the spatial and temporal variability of Arctic ice thickness on long timescales with the ice model of *Flato and Hibler* [1992] applied to the period 1951–1990. All these studies show the high interannual variability of the ice thickness. However, these authors do not calculate the sea ice volume flux through Fram Strait.

A comparison with observed sea ice fluxes is required to verify and optimize the numerical simulations. Observations of ice transports are available for some selected regions for the last few years. These data are usually derived from observations of sea ice drift, extent, percentage of areal coverage, and thickness obtained from different sensors with different spatial and temporal resolution. A review of existing observations and simulations for the Arctic climate system is given by *Barry et al.* [1993].

Wadhams [1983] gives one of the first estimates of Fram Strait ice export based on observations. He calculates a volume flux of 6200 km^3 per year, or 0.29 Sv. This value is much higher than more recent estimates. One reason for the difference is *Wadham*'s [1983] assumption of a relatively high ice thickness of 4.06 m, while the measurements of *Vinje et al.* [1998] show a 4-year mean cross-strait ice thickness of only 2.60 m.

Aagaard and Carmack [1989] estimate the magnitude of sea ice transport through Fram Strait as about 0.1 Sv. The mean export in the present simulation (0.086 Sv), which does not cover the same period, is 14% smaller. As the model has a standard deviation of 18% for the annual means 1986–1992 due to the high natural variability of the sea ice transport, the simulation results are well in the range of the estimate of *Aagaard and Carmack* [1989].

Vinje and Finnekåsa [1986] derive a transport of about 5000 km^3 per year, or 0.16 Sv, across 81°N for 1976–1984. However, this relies on an assumed ice thickness of 3.65 m, which later had to be corrected by a factor of 0.7 (T. Vinje, personal communication, 1997). The new, corrected value of about 3500 km^3 per year, or 0.11 Sv, is in fair agreement with the simulation. *Vinje et al.* [1998] estimate a mean ice transport of 2843 km^3 per year, or 0.09 Sv. This estimate is based on velocities derived from satellite images for 1993-1995 and buoy velocities for 1976-1994, and ice maps and upward-looking sonar ice thickness measurements for 1990-1996. They also find a strong year-to-year variation up to about 130%, indicating that absolute values of transports are only comparable if they cover the same period. A relatively high transport of 4687 km^3 per year, or 0.145 Sv, is estimated for 1994-1995, while their value for 1990-1991 is only 2046 km^3 per year, or 0.065 Sv.

Martin [1996] derives the ice transport through Fram Strait from satellite measurements of ice concentrations and drift velocities. Ice thickness, for which measurements were not available for this study, had to be assumed. The mean ice volume flux through Fram Strait at about 79° has been estimated as 0.068 Sv for the period 1993–1994 with an assumed mean ice thickness of 3 m. This value for 1993–1994 is about 20% smaller than the simulated long-term value for 1986–1992. *Martin* [1996] also determines the seasonal cycle of the ice transport. He calculates mean values for the four seasons (January–March, April–June, July–September, October–December) considering all data from 1993 and 1994. He finds (p. 103) that "during the summer months the flux is reduced by a factor of ten compared to the autumn in the area of Fram Strait". This result agrees well with the simulated seasonal cycle shown in Figure 8 where the summer values of ice export are smaller by an order of magnitude compared with the winter situation.

7. Discussion and Conclusions

A numerical simulation of sea ice transport through Fram Strait is integrated for the seven years 1986–1992. Interannual variability and sensitivity to atmospheric forcing, both of which are only sparsely covered by observational data, are investigated with a dynamic-thermodynamic sea ice model.

The simulation shows a high interannual variation of ice transports on timescales of months and years, caused by fluctuations in the wind field. A standard deviation of 21% is predicted for the annual means of ice export. In years with high exports, the exported sea ice amounts to twice the value of that in years with small exports.

This sea ice transport through Fram Strait is the second largest freshwater flux on Earth, affecting the freshwater input into the North Atlantic and therefore the global climate dynamics. *Aargaard and Carmack* [1989] point out that a sea ice outflow increased by 25% out of the Arctic Ocean for a period of 2 years would be sufficient to establish a freshwater anomaly as large as the Great Salinity Anomaly [e.g., *Dickson et al.*, 1988; *Legutke*, 1991] that could be traced for a decade. The simulations show that even within the range of normal variability, anomalies half as large are a regular part of the natural variability of the climate system. Larger anomalies should occur with less but still recognizable frequency. As far as sea ice transport is concerned, the model results suggest that variations in freshwater fluxes, as the Great Salinity Anomaly, are regular phenomena of fluctuations on decadal timescales.

Walsh and Johnson [1979] analyze Arctic sea ice fluctuations for 1953–1977 and describe the variability of the ice cover with empirical orthogonal functions. *Walsh and Chapman* [1990] calculate a statistically significant correlation between sea ice anomalies in the Greenland Sea and surface pressure anoma-

lies. They find that two almost independent pressure anomalies are responsible for sea ice anomalies in the Greenland Sea: the local forcing by pressure anomalies in southern Greenland and the large-scale sea ice circulation forced by pressure anomalies in the central Arctic. *Walsh and Chapman* [1990] suggest that events like the "Great Salinity Anomaly" are caused by a coincidence of both pressure anomalies simultaneously acting in the same direction. They explain the "Great Salinity Anomaly" by an extraordinarily large pressure anomaly in the late 1960s, but they also find somewhat smaller but still important anomalies in the early 1940s and 1980s. This might support the hypothesis that events like the "Great Salinity Anomaly" are regular phenomena of natural variability.

The high interannual variability in the simulations suggests that special care should be taken that all observations entering estimates of sea ice transports originate from the same time period. The strongly fluctating wind field and the associated, mainly wind-driven ice drift are especially important for calculations of ice transports. Using estimates of wind stress from different time periods may result in large errors.

For a better validation of the model results, new measurements of ice transport through Fram Strait (T. Vinje, personal communication, 1997) will be compared with the simulations. This model validation is part of the Sea Ice Model Intercomparison Project [*Lemke et al.*, 1997], with the first results shown by *Kreyscher et al.* [1997]. Longer periods of atmospheric forcing are now becoming available from the reanalyses of NCEP/NCAR and ECMWF and enable better estimates of the variability of the climate system on different timescales [*Harder et al.*, 1997].

Sensitivity studies have been performed to investigate the influence of changes in atmospheric forcing to sea ice transports. Wind and ocean current speed, air temperature, and precipitation rate have been varied over a wide range. The simulation results show a strong, almost linear dependence of sea ice export on wind and ocean current speed, a negative, nonlinear relation between air temperature and ice export, and a rather weak, negative correlation between precipitation and ice exports.

This result emphasizes the need to include dynamics, in addition to thermodynamics, in investigations and numerical simulations of the global climate system. The response of sea ice transports to changes in wind speed is of the same order as the response to changes in air temperatures. It is therefore necessary not only to estimate the amount of global warming due to natural or anthropogenic modifications of the current climate state, but also to predict the dynamics of modified wind fields and their effect on the ocean surface and global transports.

Regarding the representation of sea ice in climate models, only models including sea ice dynamics are capable of representing the large fluxes of freshwater and latent heat associated with sea ice drift. The simulations show that the magnitude of these transports is of considerable importance in driving the global climate system, and that changes in other components of the climate system cause considerable responses of the cryosphere. Thus, realistic climate simulations require a representation of both the dynamics and the thermodynamics of sea ice.

Acknowledgments. Thanks are due to G. M. Flato for processing the oceanic forcing obtained from W. D. Hibler III and J. Zhang. Ch. Kottmeier and G. König-Langlo kindly provided measurements from ice buoys and from R/V *Polarstern* run by the Alfred-Wegener-Institut für Polar- und Meeresforschung, Bremerhaven, Germany. The daily atmospheric forcing was derived from the global analyses of the European Centre for Medium-Range Weather Forecasts (ECMWF).

References

Aagaard, K., and E. C. Carmack, The role of sea ice and other fresh water in the Arctic circulation, *J. Geophys. Res.*, *94*(C10), 14485–14498, 1989.

Barry, R. G., M. C. Serreze, J. A. Maslanik, and R. H. Preller, The Arctic sea ice–climate system: Observations and modelling, *Rev. Geophys.*, *31*(4), 397–422, 1993.

Bourke, R. H., and A. S. McLaren, Contour mapping of Arctic Basin ice draft and roughness parameters, *J. Geophys. Res.*, *97*(C11), 17715–17728, 1992.

Chapman, W. L., W. J. Welch, K. P. Bowman, J. Sacks, and J. E. Walsh, Arctic sea ice variability: Model sensitivities and a multidecadal simulation, *J. Geophys. Res.*, *99*(C1), 919–935, 1994.

Colony, R., I. Appel, and I. Rigor, Surface air temperature observations in the Arctic Basin, *Tech. Memo. APL-UW TM 01-92*, Appl. Phys. Lab., Laurel, Md., July 1992.

Dickson, R. R., J. Meincke, S.-A. Malmberg, and A. J. Lee, The "Great Salinity Anomaly" in the northern Atlantic 1968–1982, *Progr. Oceanogr.*, *20*, 103–151, 1988.

Drinkwater, M. R., H. Fischer, M. Kreyscher, and M. Harder, Comparison of seasonal sea-ice model results with satellite microwave data in the Weddell Sea, paper presented at the IGARSS Conference 1995 on Recent Advances in Remote Sensing/Modelling of Sea Ice, Int. Geosci. and Remote Sens. Symp., Florence, Italy, 1995.

Ebert, E. E., and J. A. Curry, An intermediate one-dimensional thermodynamic sea ice model for investigating ice-atmosphere interactions, *J. Geophys. Res.*, *98*(C6), 10085–10109, 1993.

Fischer, H., Vergleichende Untersuchungen eines optimierten dynamisch-thermodynamischen Meereismodells mit Beobachtungen im Weddellmeer, *Ber. Polarforsch. 166*, Alfred-Wegener-Inst. für Polar- und Meeresforsch., Bremerhaven, Germany, 1995.

Fischer, H., and P. Lemke, On the required accuracy of atmospheric forcing fields for driving dynamic-thermodynamic sea ice models, in *The Polar Oceans and Their Role in Shaping the Global Environment, Geophys. Monogr. Ser.*, vol. 85, pp. 373–381, AGU, Washington, D.C., 1994.

Flato, G.M., Spatial and temporal variability of Arctic ice thickness, *Ann. Glaciol.*, *21*, 323-329, 1995.

Flato, G. M., and W. D. Hibler III, Modeling pack ice as a cavitating fluid, *J. Phys. Oceanogr.*, *22*, 626–651, 1992.

Fleming, G. H., and A. J. Semtner, Jr., A numerical study of interannual ocean forcing on Arctic sea ice, *J. Geophys. Res.*, *96*(C3), 4589–4603, 1991.

Häkkinen, S., An Arctic source for the Great Salinity Anomaly: A simulation of the Arctic ice-ocean system for 1955–1975, *J. Geophys. Res., 98*(C9), 16397–16410, 1993.

Häkkinen, S., and G. L. Mellor, Modeling the seasonal variability of a coupled Arctic ice-ocean system, *J. Geophys. Res., 97*(C12), 20285–20304, 1992.

Harder, M., Erweiterung eines dynamisch-thermodynamischen Meereismodells zur Erfassung deformierten Eises, *Ber. Fachbereich Phys. 50*, Alfred-Wegener-Inst. für Polar- und Meeresforsch., Bremerhaven, Germany, 1994.

Harder, M., Dynamik, Rauhigkeit und Alter des Meereises in der Arktis — Numerische Untersuchungen mit einem großskaligen Modell, *Ber. Polarforsch. 203*, Alfred-Wegener-Inst. für Polar- und Meeresforsch., Bremerhaven, Germany, 1996.

Harder, M., Roughness, age and drift trajectories of sea ice in large-scale simulations and their use in model verifications, *Ann. Glaciol.*, in press, 1997.

Harder, M., and P. Lemke, Modelling the extent of sea ice ridging in the Weddell Sea, in *The Polar Oceans and Their Role in Shaping the Global Environment, Geophys. Monogr. Ser.*, vol. 85, pp. 187–197, AGU, Washington, D.C., 1994.

Harder, M., M. Hilmer, and P. Lemke, Variability of Arctic sea ice thickness, in *Proceedings, ACSYS Sea Ice Thickness Workshop, Monterey 1997*, edited by R. Colony, WCRP report, WMO, Geneva, in press, 1997.

Hibler, W. D., III, A dynamic thermodynamic sea ice model, *J. Phys. Oceanogr., 9*(4), 815–846, 1979.

Hibler, W. D., III, and J. Zhang, On the effect of ocean circulation on Arctic ice-margin variations, in *The Polar Oceans and Their Role in Shaping the Global Environment, Geophys. Monogr. Ser.*, vol. 85, pp. 383–397, AGU, Washington, D. C., 1994.

Hilmer, M., Numerische Untersuchungen des Einflusses atmosphärischer Antriebsfelder in Simulationen der Grenzfläche Atmosphäre–Eis–Ozean in der Arktis, master thesis, 71 pp., Inst. für Meereskunde, Kiel, Germany, 1997.

Holland, D. M., L. A. Mysak, D. K. Manak, and J. M. Oberhuber, Sensitivity study of a dynamic thermodynamic sea ice model, *J. Geophys. Res., 98*(C2), 2561–2586, 1993.

Kreyscher, M., M. Harder, and P. Lemke, First results of the Sea Ice Model Intercomparison Project (SIMIP), *Ann. Glaciol.*, in press, 1997.

Legutke, S., Numerical experiments relating to the "Great Salinity Anomaly" of the seventies in the Greenland and Norwegian seas, *Prog. Oceanogr., 27*, 341–363, 1991.

Lemke, P., W. D. Hibler, III, G. M. Flato, M. Harder, and M. Kreyscher, On the improvement of sea ice models for climate simulations: The Sea Ice Model Intercomparison Project (SIMIP), *Ann. Glaciol.*, in press, 1997.

Martin, T., Sea ice drift in the East Greenland Current, in *Proceedings, Fourth Symposium on Remote Sensing of the Polar Environments, Eur. Space Agency Spec. Publ., ESA SP-391*, 101–105, 1996.

McLaren, A. S., R. H. Bourke, J. E. Walsh, and R. L. Weaver, Variability in sea-ice thickness over the north pole from 1958 to 1992, in *The Polar Oceans and Their Role in Shaping the Global Environment, Geophys. Monogr. Ser.*, vol. 85, pp. 363-371, AGU, Washington, D.C., 1994.

McPhee, M. G., The effect of the oceanic boundary layer on the mean drift of pack ice: Application of a simple model, *J. Phys. Oceanogr., 9*, 388–400, 1979.

Owens, W. B., and P. Lemke, Sensitivity studies with a sea ice-mixed layer-pycnocline model in the Weddell Sea, *J. Geophys. Res., 95*(C6), 9527–9538, 1990.

Parkinson, C. L., and W. M. Washington, A large-scale numerical model of sea ice, *J. Geophys. Res., 84*(C1), 311–337, 1979.

Semtner, A. J., Jr., A model for the thermodynamic growth of sea ice in numerical investigations of climate, *J. Phys. Oceanogr., 6*(3), 379–389, 1976.

Tucker, W. B. III, A. J. Gow, and W. F. Weeks, Physical properties of summer ice in Fram Strait, *J. Geophys. Res., 92*(C7), 6787–6803, 1987.

Vinje, T., and Ø. Finnekåsa, The ice transport through the Fram Strait, *Rep. 186*, 39 pp., *Nor. Polarinst.*, Oslo, 1986.

Vinje, T., N. Nordlund, and Å. Kvambekk, Monitoring ice thickness in Fram Strait, *J. Geophys. Res.*, in press, 1998.

Vowinckel, E., and S. Orvig, The climate of the North Polar Basin, in *Climates of the Polar Regions, World Surv. Climatol. Ser.*, vol. 14, pp. 129-252, edited by S. Orvig, Elsevier, New York, 1970.

Wadhams, P., Sea ice thickness distribution in Fram Strait, *Nature, 305*, pp. 108–111, 1983.

Wadhams, P., Sea ice thickness changes and their relation to climate, in *The Polar Oceans and Their Role in Shaping the Global Environment, Geophys. Monogr. Ser.*, vol. 85, pp. 337–361, AGU, Washington, D.C., 1994.

Walsh, E. J., and W. L. Chapman, Arctic contribution to upper-ocean variability in the North Atlantic, *J. Clim., 3*, 1462–1473, 1990.

Walsh, E. J., and C. M. Johnson, An analysis of Arctic sea ice fluctuations, 1953-77, *J. Phys. Oceanogr., 9*, 580–591, 1979.

Walsh, E. J., W. D. Hibler III, and B. Ross, Numerical simulation of northern hemisphere sea ice variability, *J. Geophys. Res., 90*(C3), 4847–4865, 1985.

M. Harder, M. Hilmer, and P. Lemke, Institut für Meereskunde an der Universität Kiel, Düsternbrooker Weg 20, 24105 Kiel, Germany. (e-mail: mharder@ifm.uni-kiel.de)

(Received July 19, 1996; revised July 21, 1997; accepted August 29, 1997.)